

# Change in Model Morphology Evaluated Throughout the Modeling Process of Human Trabecular Bone to Identify and Quantify Sources of Error in Methodology

McKinley Van Klei, Alexander Hadwen, Lauren Windover, Roxolana Smyk, Heidi-Lynn Ploeg  
Queen's University, Kingston, ON, Canada  
Department of Mechanical and Materials Engineering, Queen's University, Kingston, ON, Canada  
Centre for Health Innovation, Queen's University, Kingston, ON, Canada  
18msmv@queensu.ca

Disclosures: McKinley Van Klei (N), Alexander Hadwen (N), Lauren Windover (N), Roxolana Smyk (N), Heidi-Lynn Ploeg (N)

**INTRODUCTION:** Improvement in treatments for bone diseases such as osteoporosis and osteoarthritis requires further understanding of the biological and mechanical behavior of trabecular bone; located in vertebrae and epiphyses of long bones, and therefore found at the bone implant interface for joint replacements [1]. The three most common reasons for patients requiring hip and knee replacement revision surgeries are infection, aseptic loosening, and instability, emphasizing the need for research that describes mechanical behavior of bone that contributes to these complications [2]. This study aimed to analyze changes in morphology of human trabecular bone models throughout the modeling process to identify and quantify sources of error in the methodology used to construct STL files for finite element analysis (FEA) and 3D printed models.

**METHODS:** Human trabecular bone at the femoral head was donated by 2 patients (one female, one male) and cut into 48 bone cores (10 mm x 5 mm) (Figure 3). Bone core microarchitecture was captured with micro computed tomography ( $\mu$ -CT) scans (VECTor<sup>4</sup>CT; 20 $\mu$ m, 50kVp, 430 $\mu$ A, step angle 0.1°, 100ms exposure time per step). The resulting DICOM files were segmented to create 2D masks (>1100 HU) and 3D models (Materialise Mimics 24.0). The 3D model meshes were reduced (Materialise 3-Matic 24.0), exported as STL files. For 32 bone cores, the STL files were used to make 2:1 scale 3D printed models (Objet 30 Prime, RGD 525) (Figure 3). Nine of the real bone cores were cleaned to remove soft tissue; seven effectively, and two ineffectively. Bone volumes were measured (Mettler Toledo Analytical Balance) for the seven bone cores that were cleaned effectively and for 32 3D prints. A control group was established by 3D printing two STL files of simple geometry of similar volume to the bone cores. Incremental steps within the modeling process (Steps 1-4) were defined, where change in volume could be calculated. Step 1: from real bone core to 2D mask. Step 2: from 2D mask to 3D model. Step 3: from 3D model to 3D model with reduced mesh. Step 4: from 3D model with reduced mesh to 3D print. The overall process was defined as total change in morphology from the real bone core to the 3D print (n=7) (Figure 3). Nonparametric Kruskal-Wallis and Dunn's Post-Hoc statistical tests were performed to compare percent change in volume.

**RESULTS:** To evaluate change in morphology of the bone core models at each incremental step in the modeling process, the percent change in bone core volume was calculated (Step 1: median 4.88%, IQR 3.42%; Step 2: median -0.26%, IQR 0.15%; Step 3: median -0.22, IQR 0.25%; Step 4: median 14.7, IQR 11.3%; overall process: median 22.1%, IQR 17.8) (Figure 1). A statistically significant Kruskal-Wallis ANOVA ( $p = 1.22 \times 10^{-5}$ ) and Dunn's post-hoc test showed a statistically significant difference in percent change in volume between Step 1 and Step 2, Step 1 and the overall process, Step 2 and Step 4, Step 2 and the overall process, Step 3 and Step 4, as well as Step 3 and the overall process. As shown in Figure 2, the percent change in volume between the STL file used to construct the 3D print and the 3D printed model was calculated (bone core models: median 12.5%, IQR 15.3%; control: median -4.88%, IQR 2.43%). The Kruskal-Wallis ANOVA performed ( $\alpha = 0.05$ ) found a statistically significant difference between the this change in model volume of the bone core models and the control ( $p = 0.04$ ).

**DISCUSSION:** Previous studies have shown that trabecular plates and rods are between 50-200  $\mu$ m [2]. Given this, the resolution of the images captured with the  $\mu$ -CT used (VECTor<sup>4</sup>CT; 20  $\mu$ m, 50 kVp, 430  $\mu$ A, step angle 0.1°, 100 ms exposure time per step) should be sufficient to capture the unique trabecular structures. Therefore, it was concluded that the volume measurement error contributed more to the percent change in volume in Step 1 than the segmentation or  $\mu$ -CT resolution. The percent change in model volume in Step 4 is due to inaccuracies of the volume measurements and limited ability of the 3D printer in capturing complex trabecular geometry due to printer resolution. This further supports the conclusion that printer resolution negatively impacted the geometric accuracy of the 3D printed models. Results from this study are most relevant to modeling human trabecular bone at the femoral head given that trabecular geometry is site specific and mechanical behavior varies with anatomical location.

**SIGNIFICANCE/CLINICAL RELEVANCE:** Identification and quantification of sources of error within the modelling process for computational and 3D printed models of human trabecular bone will contribute to improvement of geometrically accurate trabecular bone models. Establishing trabecular bone FEA models that can accurately predict bone fragility and stress and strain fields will improve patient outcomes for complications related to bone disease.

## REFERENCES:

- [1] Ramin O., Miguel P., *et al.* Biomechanics and Mechanobiology of Trabecular Bone: A Review. *J Biomech Eng* (2015)
- [2] Canadian Joint Replacement Registry (CJRR) *et al.* Hip and Knee Replacements in Canada *CJRR Annual Report* (2022)

**ACKNOWLEDGEMENTS:** We would like to acknowledge Leone Ploeg for her work with the Centre for Health Innovation, Luisa Meyer for her work at the University of Wisconsin-Madison on trabecular bone modeling, and Elahe Alizadeh for her work with the Queen's Cardio-Pulmonary Unit and micro-CT scanning expertise.

## IMAGES AND TABLES:

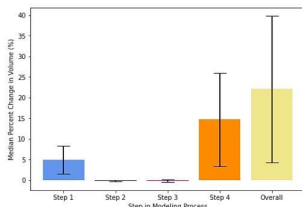


Figure 1: Median percent change in bone core volume for isolated steps in modeling process and overall process, from the real bone core to the corresponding 3D Print (n = 7). Whiskers show inter-quartile range (IQR).

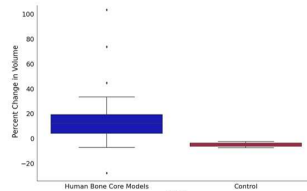


Figure 2: Percent change in volume for Step 4 of modeling process, from the 3D model (STL file) to the 3D print, for bone cores (n = 32) and control group (n = 2). Whiskers show inter-quartile range and outliers are indicated with individual plotted points.



Figure 3: Real bone core (right) and corresponding 3D printed model (left).